INTERNATIONAL JOURNAL OF CIVIL ENGINEERING AND TECHNOLOGY (IJCIET)

ISSN 0976 – 6308 (Print)
ISSN 0976 – 6316(Online)
Volume 5, Issue 10, October (2014), pp. 104-123

Journal Impact Factor (2014): 7.9290 (Calculated by GISI)
www.jifactor.com

IJCIET

©IAEME

APPLICABILITY OF MOHR-COULOMB & DRUCKER-PRAGER MODELS FOR ASSESSMENT OF UNDRAINED SHEAR BEHAVIOUR OF CLAYEY SOILS

Sandhya Rani. R.[1], Nagendra Prasad. K[2]., Sai Krishna. T.[3]

[1](Research Scholar, Dept. of Civil Engineering, SV University, Tirupati, India)
[2](Professor of Civil Engineering, SV University, Tirupati, 517502, AP, India)
[3](Former Post Graduate Student, Dept. of Civil Engineering, SV University, Tirupati, India)

ABSTRACT

Properties of soils and the techniques to determine the same are very much dependent on the local geological conditions and the environment. The scope of the present study includes understanding the model predictions from classical constitutive models such as Mohr-Coulomb & Drucker-Prager. These models are widely used despite availability of advanced models vowing to simplicity and easily determinable model parameters. An attempt has been made to present the formulation of the stress integration procedure for Mohr-Coulomb and Drucker-Prager models with associative yielding condition by using the incremental plastic theory which is a conventional and convenient practice in drawing stress paths. Stress dependent moduli are used for the purpose. To check the applicability of these models, experimental values from published data are compared with the model predictions. The parameters involved are same as Cam clay model parameters which are simple and easily determinable from the experimental results performed in routine soil investigations. By making the comparative study, the salient features that can be captured are understood for appropriate use in engineering applications. The undrained situation which is realistic in clayey soils is used in the present work. It is observed that the Mohr- Coulomb Model shows lower predictions compared to Drucker-Prager Model. These are the deviations observed with the stress-strain response of the results, in that the strength predictions being similar, the elasto-plastic response & the critical state conditions are different.

Keywords: Constitutive Models, Clayey Soils, Mohr-Coulomb, Drucker-Prager, Critical State.

International Journal of Civil Engineering and Technology (IJCIET), ISSN 0976 – 6308 (Print), ISSN 0976 – 6316(Online), Volume 5, Issue 10, October (2014), pp. 104-123 © IAEME

1. INTRODUCTION

There are many problems related to the soil in geotechnical field such as bearing capacity of shallow and deep foundations, slope stability, retaining wall design, penetration resistance, soil liquefaction, etc. These problems are affected by the soil properties; the most influence property is the shear strength of the soil. Analytical and numerical analyses use values of shear strength for solving these engineering problems and monitoring the performance of real structures. The studies of soil behaviour is very important and useful for design works, construction practices and for collecting and gaining more information that can be used in the design of structures that could be constructed on residual soils.

2. BACKGROUND INFORMATION

Linear elastic-perfect plasticity using the Mohr-Coulomb yield surface is one of the most widely used pressure- sensitive constitutive models in engineering practice. In the area of geotechnical engineering, a number of problems, such as cavity expansion, embankment stability, and footing bearing capacity, can be examined using this model together with the simplifying assumption of plane strain. The linear elastic-perfectly plastic Mohr-Coulomb (M-C) model is one of the most widely used pressure-sensitive constitutive models, which can capture this behaviour in an idealized way (Coombs et al, 2013).

The constitutive laws for the isotropic linear elastic-perfectly plastic M-C model are widely available in the literature (Clausen et al. 2006, 2007). Established procedures for dealing with non-smooth yield surfaces are used [e.g., see Clausen et al. (2006, 2007)].Different expressions of the Mohr–Coulomb (M–C) criterion as well as the interrelationships between them, which lays a foundation for the definition of the equivalent M–C friction angle ϕ_{mc} are presented. The Druker – Prager strength criterion, called the Extended Von Mises criterion as well, has been widely used in geotechnical engineering to predict failure strength and be employed for plastic potential in continuum damage mechanic model (Wu et al., 2006; Shao et al., 2009; Voyiadjis et al., 2008).

The Mohr–Coulomb (M–C) criterion is one of the most commonly used strength theories in geotechnical engineering. However, two disadvantages of the M–C criterion limit its wider application. The first one is that the major principal stress σ_1 is independent of the intermediate principal stress σ_2 for the M–C criterion, which leads to underestimate the yield strength of material and disagrees with the test results reflecting the influence of σ_2 to the strength of material in many cases (Al-Ajmi and Zimmerman, 2005). The second one is the trace of the yield surface on deviatoric plane is an irregular hexagon which impairs the convergence in flow theory due to the six sharp corners. According to these shortcomings, some more realistic criteria have been formulated: the Twin-Shear Unified criterion (Mao-Hong et al, 2006). Recently, Griffiths and Huang (2009) proposed ϕ_{mc} for the extended Matsuoka–Nakai criterion for cohesive material, and the author introduced a new method to calculate ϕ_{mc} for cohesive and frictional material.

The Druker –Prager strength criterion, called the Extended Von Mises criterion as well, has been widely used in geotechnical engineering to predict failure strength and be employed for plastic potential in continuum damage mechanic model (Wu et al., 2006; Shao et al., 2009; Voyiadjis et al., 2008).

3. SOIL-STATE AND STRESS PARAMETERS

The state of soil is essentially the closeness of packing of the grains and depends on current vertical and horizontal effective stresses, current water content, liquidity index in case of fine-

grained soils and density index in coarse-grained soils ,history of loading and unloading, degree of over consolidation etc.,

The instantaneous two-dimensional state of stress may be represented by a Mohr's circle of stress as shown in Fig 1. The position of the Mohr's circle and its size may be identified by the coordinates (s′,t′) of its apex M′ and we could trace the loading of an element by plotting the path of M′ on axis s′ and t′. By inspection of Figure 1, it can be seen that t′ is the radius of the Mohr's circle of effective stress and is equal to the mean of σ'_x and σ'_z.

From the geometry of the Fig 1, we have

$t' = ½ [(\sigma'_x - \sigma'_z)^2 + 4\tau^2_{xz}]^{1/2}$
$s' = ½ (\sigma'_x + \sigma'_z)$

or, in terms of principal effective stresses,

$t' = ½ (\sigma'_1 - \sigma'_3)$
$s' = ½ (\sigma'_1 + \sigma'_3)$

3.1 Invariants of Stress

The parameters t′ and s′ are rather special because, for a given state of stress, their values are independent of the arbitrary choice of the orientation of the reference axes. For this reason, they are appropriate measures of the state of stress for the two dimensional stress states considered.

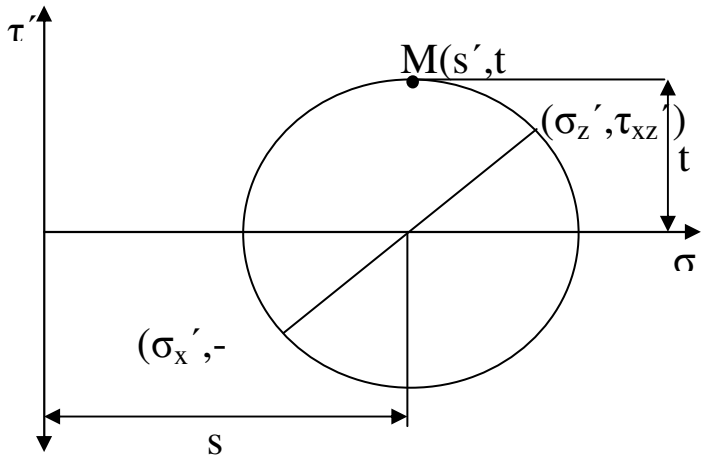

Fig: 1: Definition of stress parameters t′ and s′

Stress parameters the magnitudes of which are independent of the choice of reference axes are usually known as *stress invariants*. They are invariant in the sense that their magnitudes do not change as the reference axes are varied. The term ′stress invariant′ is strictly reserved for parameters appropriate to general states of stress and, further, that the parameters t′, s′ are not entirely satisfactory as complete measures of a two dimensional state of stress as the value of the intermediate principal stress σ'_2 has been ignored. Nevertheless, use of the parameters t′ and s′ is often convenient when, for example, the value of the intermediate principal stress is not known.

The octahedral normal effective stress σ'_{oct} and the octahedral shear stress τ'_{oct} are invariants and these are defined by

$\sigma'_{oct} = \frac{1}{3} (\sigma'_x + \sigma'_y + \sigma'_z)$
$\tau'^2_{oct} = (1/9) [(\sigma'_x - \sigma'_y)^2 + (\sigma'_y - \sigma'_z)^2 + (\sigma'_z - \sigma'_x)^2 + 6(\tau^2_{xy} + \tau^2_{yz} + \tau^2_{zx})]$

or, in terms of principal stresses,

$\sigma'_{oct} = \frac{1}{3} (\sigma'_1 + \sigma'_2 + \sigma'_3)$
$\tau'_{oct} = \frac{1}{3} [(\sigma'_1 - \sigma'_2)^2 + (\sigma'_2 - \sigma'_3)^2 + (\sigma'_3 - \sigma'_1)^2]^{1/2}$

The meaning of the parameters σ'_{oct} and τ'_{oct} is illustrated in Fig 2.

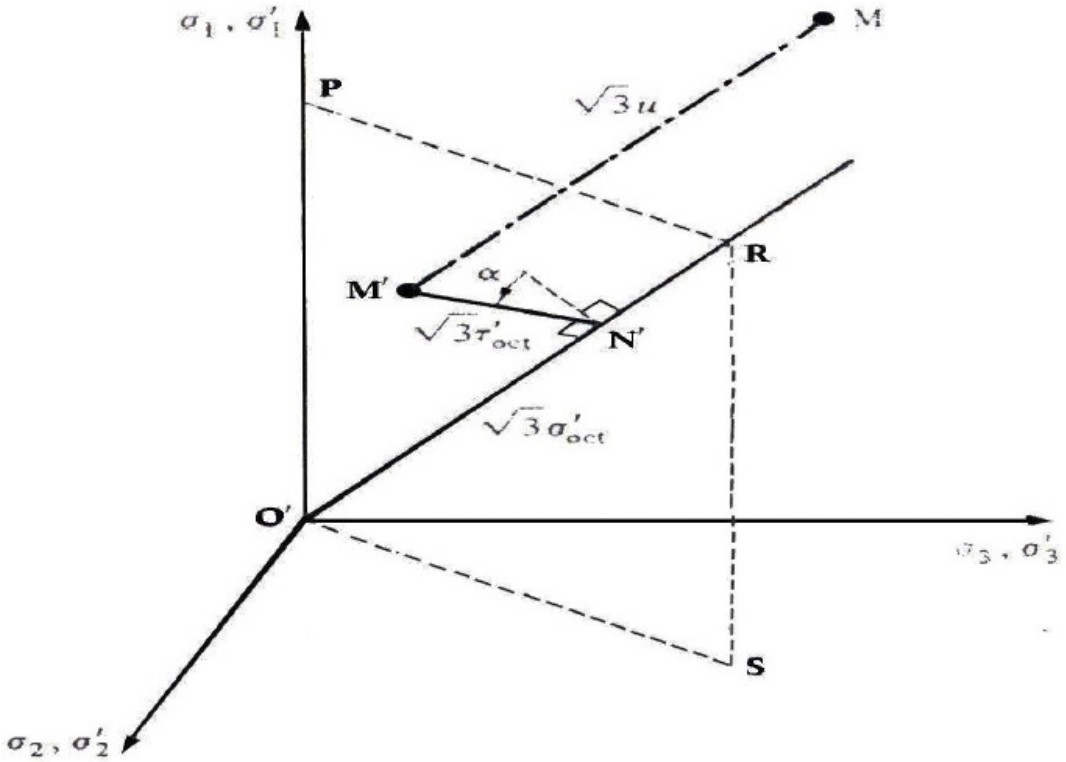

Fig: 2: Representation of octahedral stress

The state of effective stress at M′ may be described by a distance O′N′ along the space diagonal O′R together with a distance N′M′ normal to O′R; the vector O′N′ is equal to $\sqrt{3}\sigma'_{oct}$ and the vector N′M′ is equal to $\sqrt{3}\tau'_{oct}$.

For the special case of axial symmetry, where $\sigma'_2 = \sigma'_3$,

$\sigma'_{oct} = \frac{1}{3} (\sigma'_1 + 2\sigma'_3)$
$\tau'_{oct} = (\sqrt{2}/3) [(\sigma'_1 - \sigma'_3)]$
To avoid the recurring $\sqrt{2}/3$ term, we will define new invariants q′ and p′, where,

$p' = \frac{1}{3} (\sigma'_1 + 2\sigma'_3) = \sigma'_{oct}$
$q' = (\sigma'_1 - \sigma'_3) = (3/\sqrt{2})\ \tau'_{oct}$
and the corresponding strain parameters are

$\epsilon_v = (\epsilon_1 + 2\epsilon_3)$,
$\epsilon_s = (2/3) (\epsilon_1 - \epsilon_3)$

International Journal of Civil Engineering and Technology (IJCIET), ISSN 0976 – 6308 (Print), ISSN 0976 – 6316(Online), Volume 5, Issue 10, October (2014), pp. 104-123 © IAEME

3.2 Isotropic Compression

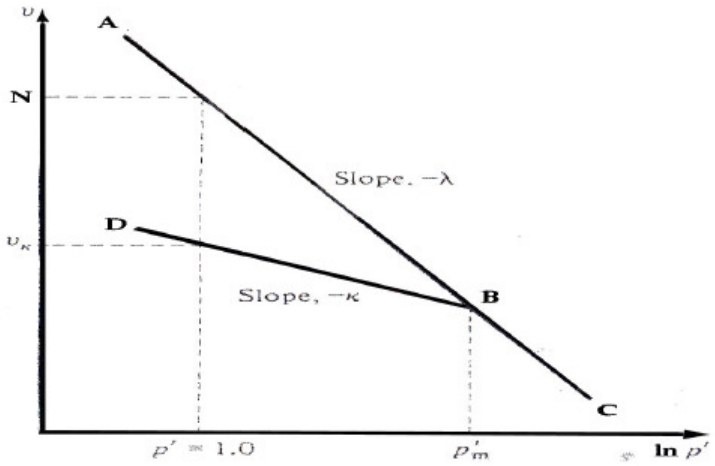

Fig 3: Isotropic compression of clay

Fig 3 is an isotropic compression diagram for a clay soil.

We define parameters λ (small lambda) and κ (small kappa) for the slopes of the normal consolidation line and a typical swelling line, respectively. Hence,
along AC,

$$-\lambda = \frac{dv}{d(\ln p')} = \frac{p'\,dv}{dp'}$$

and along BD,

$$-\kappa = \frac{dv}{d(\ln p')} = \frac{p'\,dv}{dp'}$$

Two further parameters are required to define the positions of the normal consolidation and swelling lines. For the normal consolidation line we define N (capital nu) as the specific volume of a normally consolidated soil at $p' = 1.0$ KN/m^2. Thus, the equation of the normal consolidation line is
$v = N - \lambda \ln p'$

The position of a swelling line is not unique, but depends on p'_m, the maximum previous stress. For the swelling line, we define v_κ as the specific volume of an over consolidated soil at $p' = 1.0$ KN/m^2, the equation of a swelling line is

$$v = v_\kappa - \kappa \ln p'$$

λ, N and κ are regarded as soil constants; their values will depend on the particular soil and must be found by experiment.

4. CLASSICAL MODELS

Solutions in soil constitutive modelling have been based upon Hooke's law of linear elasticity for describing soil behaviour under working loading condition and Coulomb's law of perfect plasticity for describing soil behaviour under collapse state because of its simplicity in applications. The combination and generalization of Hooke and Coulomb's law is formulated in a plasticity

framework and is known as Mohr-Coulomb model. Various constitutive models have been proposed by several researchers to describe various aspects of soil behaviour in detail and also to apply such models in finite element modelling for geotechnical engineering applications. Two basic and practical soil constitutive models such as Mohr-Coulomb and Drucker-Prager were discussed below.

4.1 Mohr-Coulomb Model

For geo materials like soils and rocks, in principal both the cohesion and the friction angle may increase (hardening) or decrease (softening) with the progress of plastic deformation and that the hardening/softening behaviours are related only to the increase/decrease of the cohesion while the internal friction remains constant during the plastic deformation (Chen, 2012).

Mohr-Coulomb model as shown in Fig 4 is an elastic-perfectly plastic model which is often used to model soil behaviour in general and serves as a first-order model. In general stress state, the model's stress-strain behaves linearly in the elastic range, with two defining parameters from Hooke's law (Young's modulus, E and Poisson's ratio, υ). There are two parameters which define the failure criteria (the friction angle, φ and cohesion, c) and also a parameter to describe the flow rule (dilatancy angle, ψ) which comes from the use of non-associated flow rule which is used to model a realistic irreversible change in volume due to shearing.

In the conventional plastic theory, the flow rule is used as the evolution law for plastic strain rates. If the plastic potential function is the same as the yield function, the flow rule is called as the associated flow rule and if it is different, it is called the non-associated flow rule. In soil mechanics, an associated flow rule has been used to model the behaviour in the region where negative dilatancy is significant, for example, the Cam clay model for normally consolidated clay.

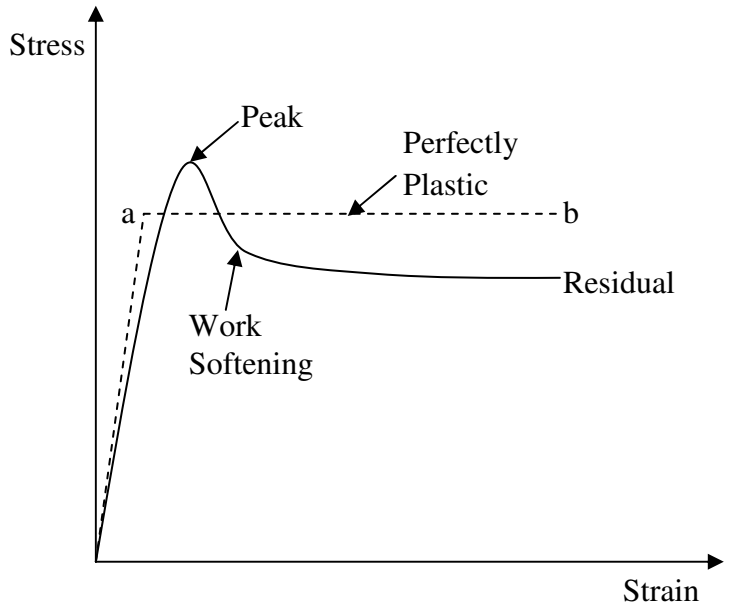

Fig 4: Elastic-perfectly plastic assumption of Mohr-Coulomb model

However, non-associated flow rule is frequently used to describe the behaviour of sands with both negative and positive dilatancy. Mohr-Coulomb model is a simple and applicable to three-dimensional stress space with only two strength parameters to describe the plastic behaviour. Regarding its strength behaviour, this model performs better.

International Journal of Civil Engineering and Technology (IJCIET), ISSN 0976 – 6308 (Print), ISSN 0976 – 6316(Online), Volume 5, Issue 10, October (2014), pp. 104-123 © IAEME

4.2 Drucker-Prager Model

The simplification of Mohr-Coulomb model where the hexagonal shape of the failure cone was replaced by a simple cone was known as the Drucker-Prager model (Drucker & Prager, 1952). Generally, it shares the same advantages and limitations with the Mohr-Coulomb model. In Drucker-Prager Model the yield is circular, from the centre to the yield surface it is equidistance.

A generalization to account for the effects of all principal stresses was suggested by Drucker and Prager by using the invariants of the stress tensor. This generalized criterion can be written as

$$f = \sqrt{J_{2D}} - \alpha J_1 - k$$

Where α and k are positive material parameters, J_1 is the first invariant of the stress tensor, and J_{2D} is the second invariant of deviatoric stress tensor.

The features of the Mohr-Coulomb and Drucker-Prager criterion are presented in Figs 5 &6. respectively.

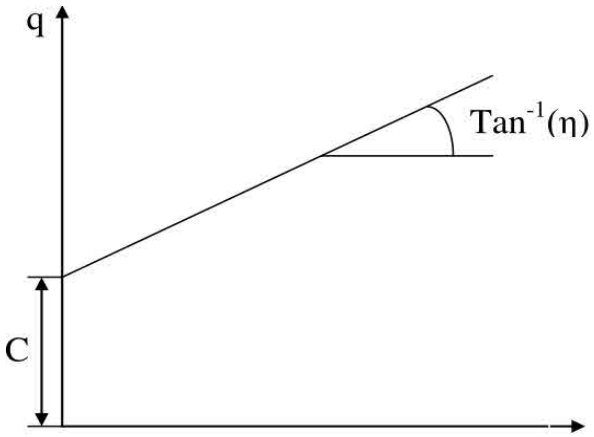

Fig 5: Mohr-Coulomb failure envelope in p-q plane

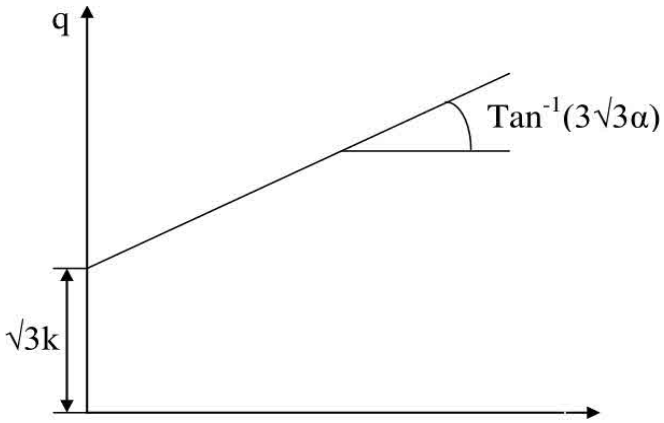

Fig 6: Drucker-Prager failure envelope in p-q plane

The values of η and C in Mohr-Coulomb criteria and the values of α and k in Drucker-Prager criteria can be expressed in terms of angle of internal friction ϕ and cohesion c as

$$\eta = \frac{6\sin\phi}{3-\sin\phi}$$

$$C = \frac{6c\cos\phi}{3-\sin\phi}$$

and,

$$\alpha = \frac{2\sin\phi}{\sqrt{3}(3-\sin\phi)}$$

$$k = \frac{6c\cos\phi}{\sqrt{3}(3-\sin\phi)}$$

For use of Mohr-Coulomb and Drucker-Prager criteria in the context of conventional incremental plasticity theory, the failure criteria are used as the yield criteria. Then the incremental stress-strain relations can be derived based on the particular yield criterion and the concepts of normality and flow described.

5. MOHR-COULOMB AND DRUCKER-PRAGER MODELS IN P-Q NOTATION

The stress invariants (i.e mean principal stress p and principal stress difference q) are used to draw the stress paths in most elasto-plastic models such as Cam clay model and it becomes a conventional practice in drawing stress paths in p-q plane. Hence, an attempt has been made to present the formulation of the stress integration procedure for Mohr-Coulomb and Drucker-Prager models. Stress integration represents calculation of stress change during an incremental step, corresponding to strain increments in the step. It is in essence the incremental integration of inelastic constitutive relationships to trace the history of material deformation (Rakic et al, 2008).

In Drucker-Prager model, the J space is converted into p-q space and the σ space is converted into p-q space in Mohr-Coulomb model. These conversions are shown in detail in Appendix. The elastic-plastic matrix is developed in p-q notation for a) Drucker-Prager model b) Mohr-Coulomb model.

Drucker-Prager Model in p-q space:

$$F(0) = \sqrt{(q^2/3)} - 3\alpha p - k$$

Mohr-Coulomb Model in p-q space:

$$F(0) = q - ((6p + q)/3)\sin\phi - 2c\cos\phi = 0$$

The only difference between Mohr-Coulomb and Drucker-Prager models is that intermediate principal stress is not considered in case of Mohr-Coulomb model. Both models assume elasticity up to failure surface & predictions obtained are elastic-plastic in nature. However since soils exhibit non-linear elasto-plastic behaviour, the bulk modulus is made a function of current state of stress as mentioned below (Atkinson& Bransbay, 1978).

$$K = vp'/\kappa$$

$$E = 3K(1-2\upsilon)$$

$$G = [3K(1-2\upsilon)] / [2(1+\upsilon)]$$

International Journal of Civil Engineering and Technology (IJCIET), ISSN 0976 – 6308 (Print), ISSN 0976 – 6316(Online), Volume 5, Issue 10, October (2014), pp. 104-123 © IAEME

6. MODEL PREDICTIONS

The undrained situation which is realistic in clayey soils is used in the present work. The model parameters in Table.1 are computed for typical values of liquid limit 40 and angle of internal friction 25^0. The model predictions by Mohr-Coulomb and Drucker-Prager represent undrained behaviour of soil for a confining pressure of 100 KPa.

Table 1: Model Parameters

Model Parameter	Value	Source
Cc (= 0.009(LL-10))	0.27	Terzaghi & Peck (1967)
λ (= Cc/2.303)	0.117	(Wood, 1990)
κ (= λ/4)	0.029	
M (= 6sinϕ/(3-sinϕ))	0.984	
e (= wG/Sr)	1.08	
v (=1+e)	2.08	
N (= v+λ ln 1)	2.08	
Γ (= N-λ+κ)	1.99	

The predictions of Drucker-Prager and Mohr-Coulomb models are shown in Fig 7. The Mohr-Coulomb model predicts lower strength at greater strains at all stages of loading compare to Drucker-Prager model.

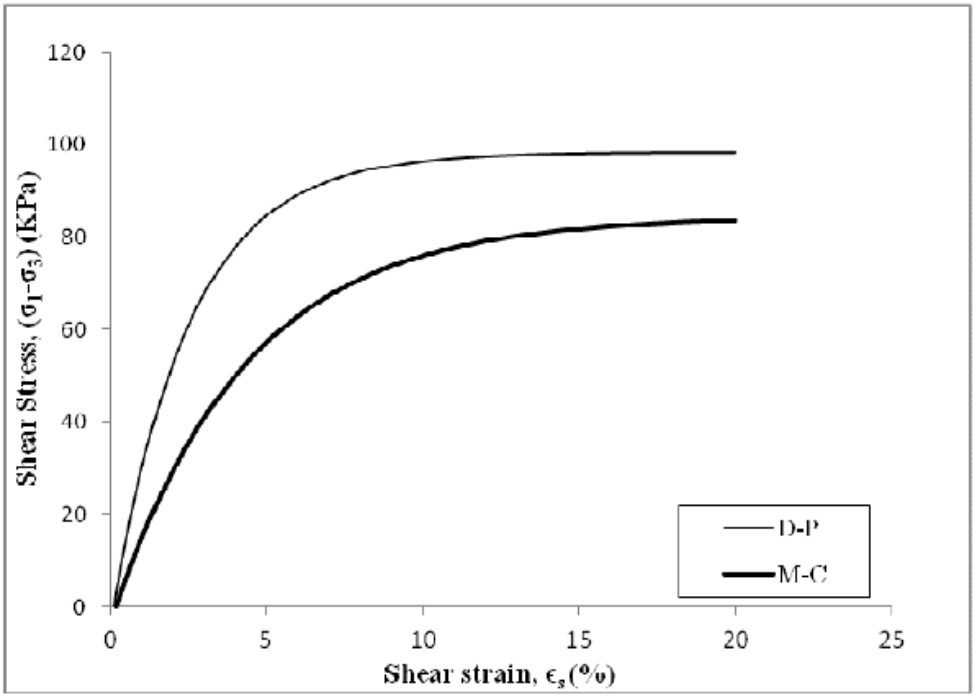

Fig 7: Predictions of Mohr-Coulomb and Drucker-Prager models

Stress-strain curves are developed for further comparison between Drucker-Prager and Mohr-Coulomb models. In order to bring out the comparison of predictions by Drucker-Prager and Mohr-Coulomb models, different values of liquid limit and corresponding estimated values of angle of internal friction are considered by keeping the other model parameters constant. The range of liquid limit considered is 40, 50, 60, 70 and 80 and the range of angle of internal friction considered is 15, 20, 25, 30 and 35.

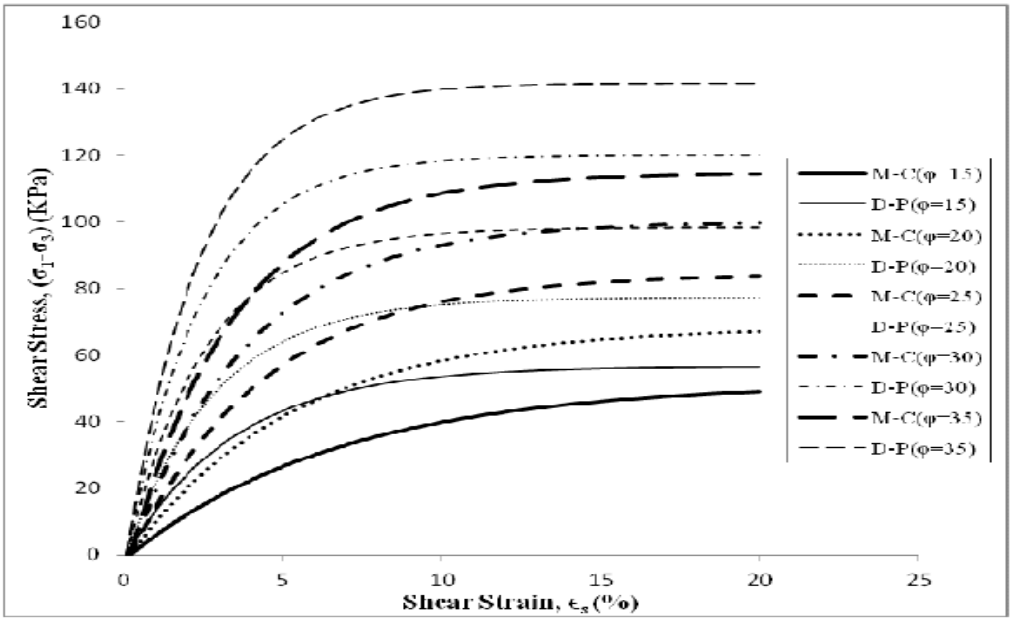

Fig 8: Stress Contours for different values of angle of internal friction at a Liquid limit of 40%

It may be seen from the Fig 8 that the strength depends on frictional mobilisation (represented by Φ) at particulate level, which in turn depends on state of the soil. For example, the soil with same liquid limit can exist at different states. Similarly, the soils with different liquid limits can have same equilibrium void ratios at different normal pressures. Alternatively, at the same normal pressure the soil with greater liquid limit may have higher equilibrium void ratio.

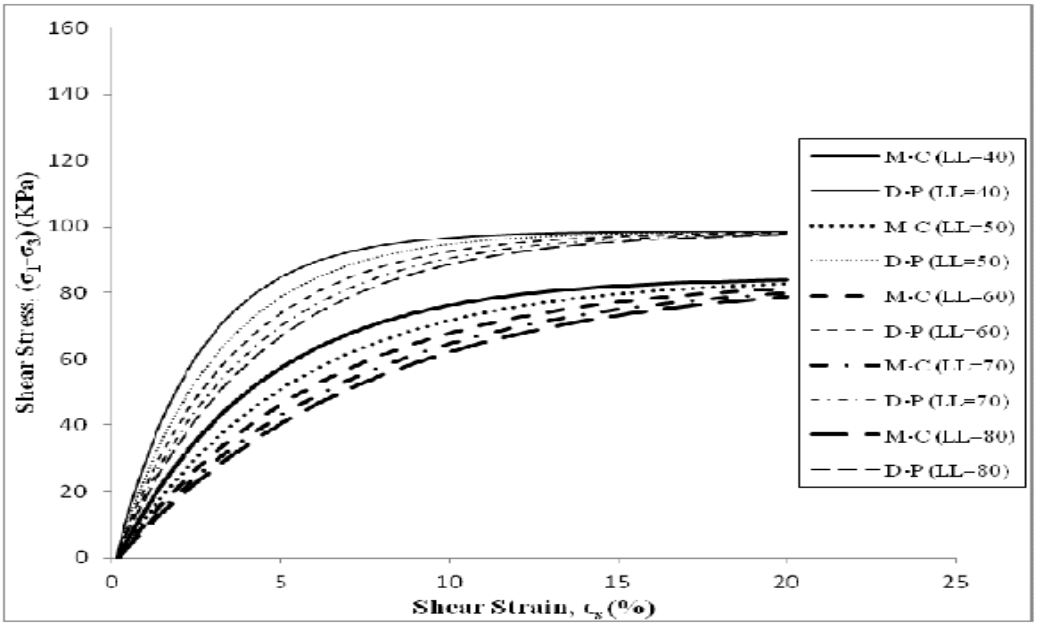

Fig 9: Stress Contours for different values of Liquid limit at an angle of internal friction of 25^o

The stress-strain response of model predictions for Drucker-Prager and Mohr-Coulomb, presented in Fig 9 clearly indicates that the strength development will be same, as long as angle of internal friction is the same. However, the stress-strain response depends on the liquid limit value. Greater the liquid limit greater will be the strain experienced by the soil to reach the strength for a given state.

International Journal of Civil Engineering and Technology (IJCIET), ISSN 0976 – 6308 (Print), ISSN 0976 – 6316(Online), Volume 5, Issue 10, October (2014), pp. 104-123 © IAEME

7. APPLICABILITY OF MODELS

An attempt has been made to apply these models to the actual soils behaviour. Soil data pertaining to different soils as presented in Table 2 are considered. It may be seen from the table that the soil types considered represent wide spectrum of properties. The clay fraction varies from 10-64%, the liquid limit values vary from 42-120 and plastic limit values vary from 20-57%. The model parameters estimated for the soils considered are shown in Table 3.

Table 2: Soil Data from Literature

Source	Suksun Horpibulsuk et al (2004)	Cheng Zhou et al (2005)	Futai et al (2004)		Burland et al (1996)	Balasubramaniam & Chaudhry (1978)
Typical Name of Soil	Ariake clay	Hong Kong Marine deposit	Lateritic soil	Saprolitic soil	Pietrafitta clay	Soft Bangkok clay
Location	Saga, Japan	Hong Kong	Ouro Preto, Brazil		Italian peninsula	Bangkok
Depth of Sampling(m)	2	10	1	5		5.5 to 6
% Sand	1	27	45	38		4
% Silt	44	43	10	52		31.7
% Clay	55	30	45	10		64.3
Specific Gravity, G_s	2.6	2.57	2.63	2.68	2.71	2.75
Natural water content (%)	150	54.3	28	46	41.9	122-130
Liquid Limit (%)	120	57	58	42	87	118±1
Plastic Limit (%)	57	25	28	20	34.5	43±0.5
Cohesion (KN/m^2)	0		7	15		0
Angle of internal friction	38^o	31.5^o	28.1^o	31^o	24.5^o	26^o

Table: 3 Model parameters obtained

Soil Type	N	λ	κ	M	υ
Ariake clay	4.82	0.43	0.11	1.54	0.43
Hong Kong Marine deposit	4.2	0.16	0.05	1.24	0.3
Lateritic soil	3.2	0.18	0.045	1.2	0.22
Saprolitic soil	2.2	0.12	0.03	1.2	0.2
Pietrafitta clay	4.6	0.12	0.03	1.13	0.2
Soft Bangkok Clay	4.8	0.12	0.03	0.69	0.2

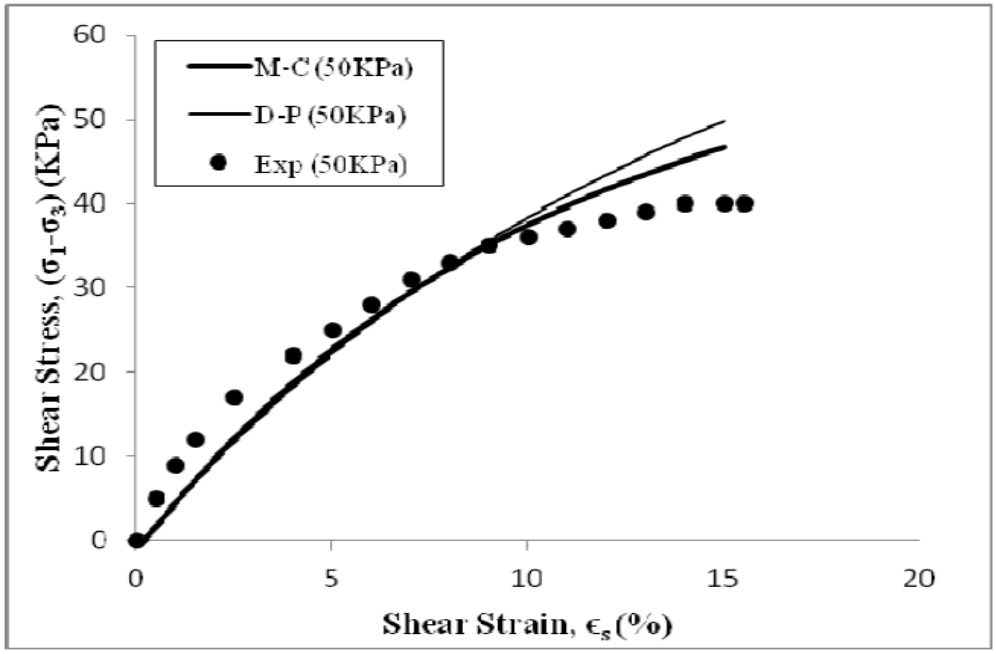

Fig 10: Comparison of model predictions and experimental results of Ariake clay (Suksun Horpibulsuk et al, 2004)

Fig 10 shows the experimental and predicted stress strain behaviour of Ariake clay. The stress-strain response predicted by the Drucker-Prager model and Mohr-Coulomb models are in agreement with the experimental observation. Fig 11 shows the experimental and predicted stress strain behaviour of Hong-Kong clay. The stress-strain response predicted by the Drucker-Prager model is in agreement with the experimental results, though the strength value matches well with the Mohr-Coulomb model predictions. As noted before the strains predicted by Mohr-Coulomb model are conservative.

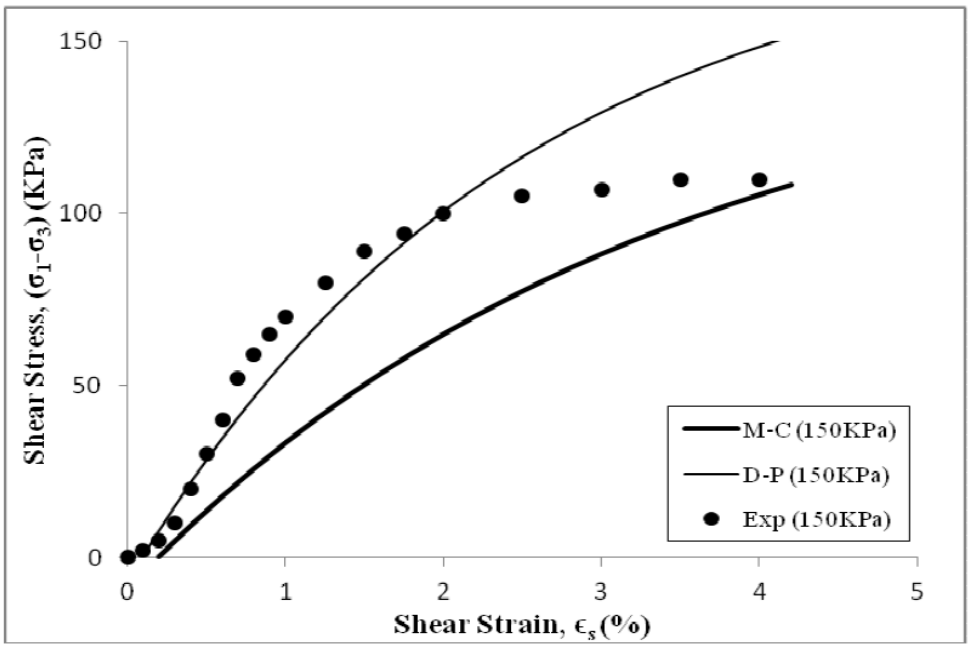

Figure 11: Comparison of model predictions and experimental results of Hong Kong clay (Cheng Zhou et al 2005)

Fig 12 and 13 show the predictions of lateritic soil and Saprolitic soil collected from different horizons of soil at same location (Futai et al,2014). It may be noticed that the features of the stress-strain response correponding to strain-softening behaviour can not be predicted by Druker –Prager and Mohr-Coulomb models . This post peak softening in soils occur due to the presence of natural cementation and structure between soil grains and was not predicted by any of these models. However these models predict only elasto-plastic response of soils. These models do not capture the strain softening behaviour which is found in natural soils. Fig 14 shows the predictions of the models for Pietrafitta clay (Burland et al 1996). The stress-strain response predicted by the Drucker-Prager model is in agreement with the experimental results; however, as noted before, the strain-softening behaviour cannot be predicted.

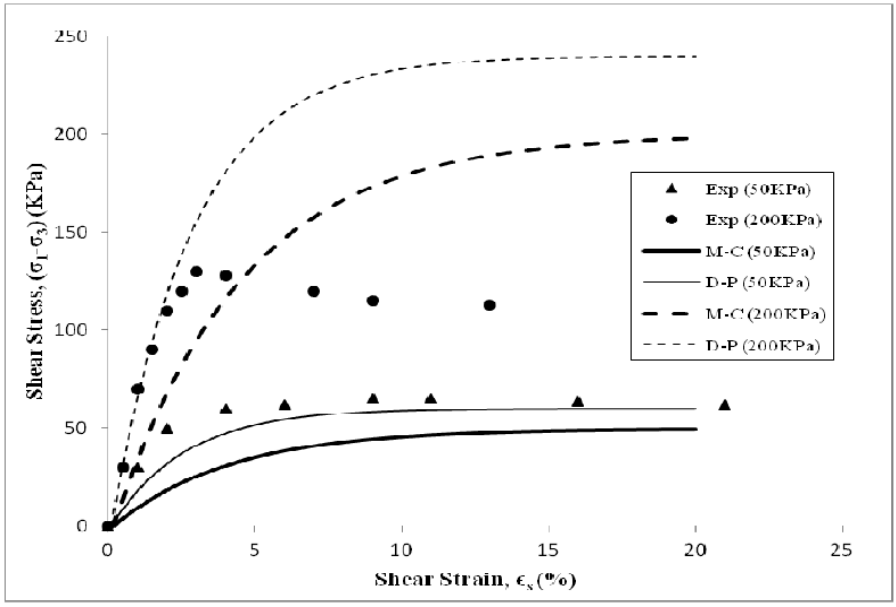

Figure 12: Comparison of model predictions and experimental results of Lateritic soil (Futai et al, 2004)

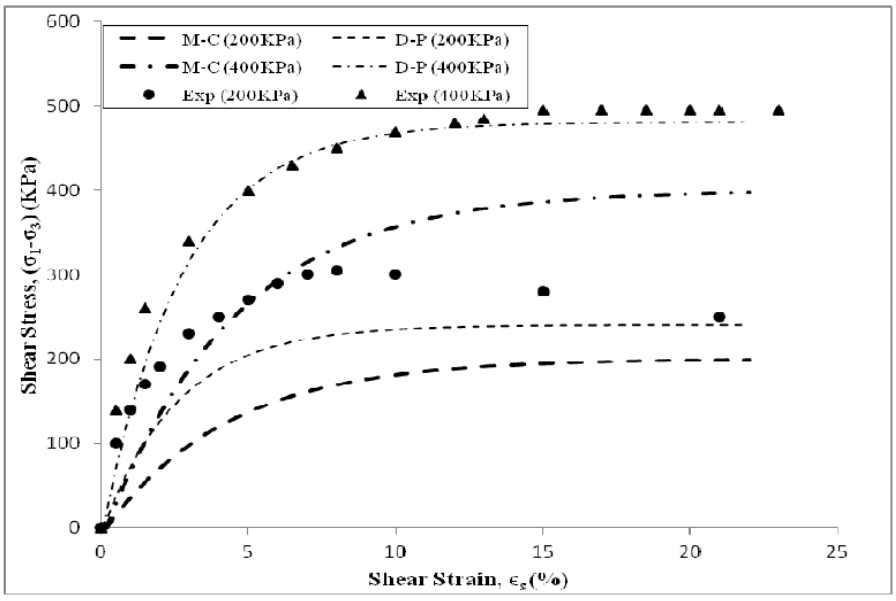

Figure 13: Comparison of model predictions and experimental results of Saprolitic soil (Futai et al, 2004)

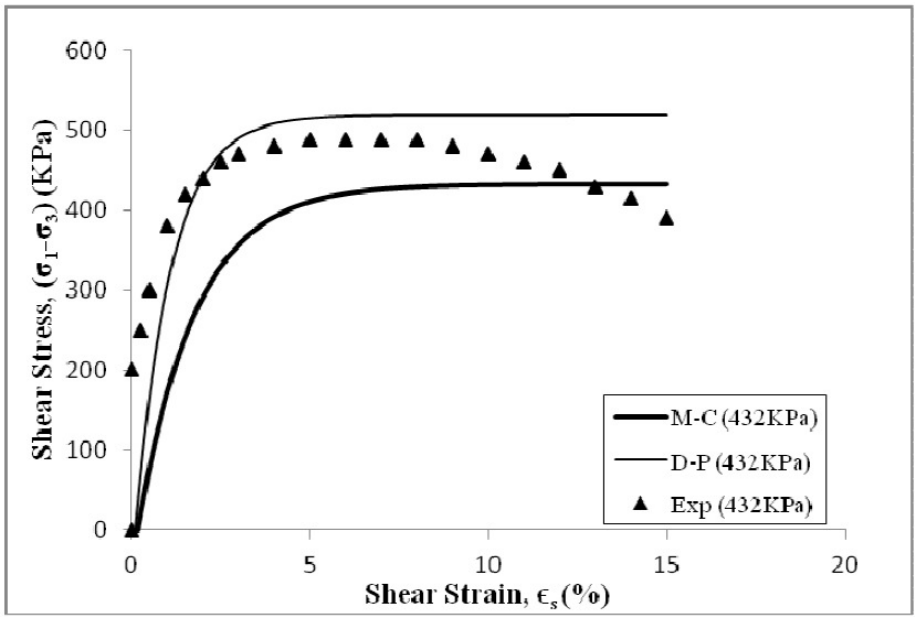

Figure 14: Comparison of model predictions and experimental results of Pietrafitta clay (Burland et al 1996)

Fig 15 and 16 show the predictions of soft Bangkok clay at different confining pressures. The stress strain behaviour of soil differs depending on the confining pressure. The soil behavior at lower and higher values of confining pressure is closely predicted by Drucker-Prager model and the rest are reasonably predicted by both the models.

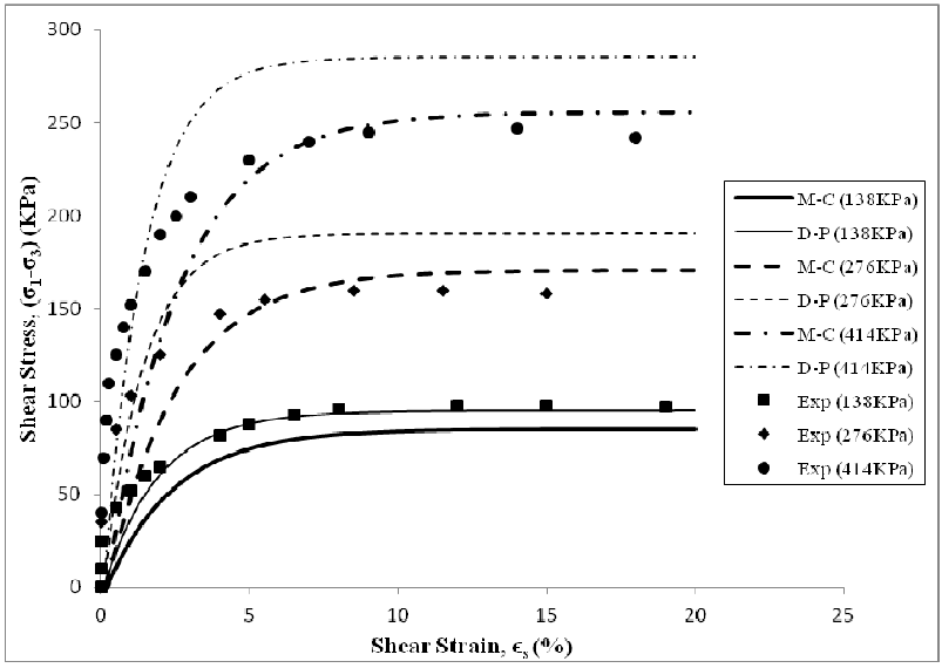

Figure 15: Comparison of model predictions and experimental results of Soft Bangkok clay (Balasubramaniam & Chaudhry, 1978)

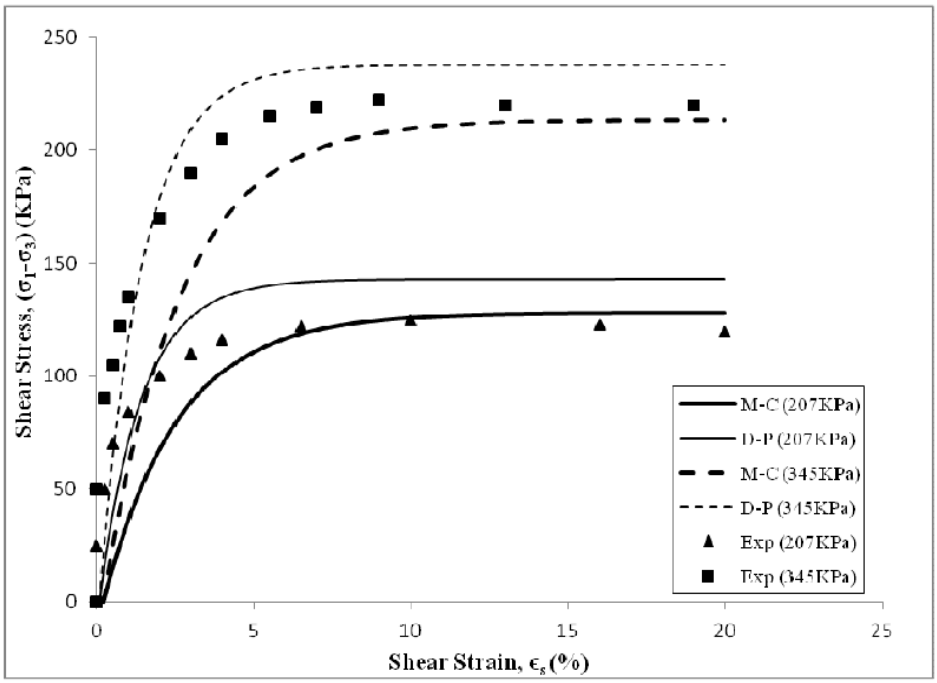

Figure 16: Comparison of model predictions and experimental results of Soft Bangkok clay (Balasubramaniam & Chaudhry, 1978)

From all the above observations, the Drucker-Prager predictions are found to be in better agreement with the experimental results. The Mohr-Coulomb predictions are conservative and hence are in vague in many practical situations in engineering practice. The soils exhibiting post peak softening, possibly due to the presence of natural structure was not predicted by any of these models.

8. CONCLUDING REMARKS

An attempt has been made to obtain the stress-strain response under undrained loading path. A limited attempt to understand the differences in predictions of the behaviour of clayey soils by Mohr-Coulomb and Drucker-Prager models as also in relation to the experimental results of soils obtained from literature. The analysis of model predictions vis-a vis experimental data permit to make the following remarks:

- The Mohr-Coulomb / Drucker-Prager models are widely used , owing to simplicity and easily determinable model parameters , in numerous engineering applications such as mining operations & other unloading situations.
- The predictions from Mohr-Coulomb model are similar to Drucker-Prager model, However Drucker-Prager model predicts greater strength at lower deformation compared to Mohr-Coulomb model.
- The Mohr-Coulomb model predicts lower strength at greater strains at all stages of loading compared to Drucker-Prager model. This is perhaps due to effect of intermediate principal stress.
- The strength depends on frictional mobilisation (represented by Φ) at particulate level, which in turn depends on state of the soil. For example, the soil with same liquid limit can exist at different states. Similarly, the soils with different liquid limits can have same equilibrium void ratios at different normal pressures. Alternatively, at the same normal pressure the soil with greater liquid limit may have higher equilibrium void ratio.

- The stress-strain response of model predictions for Drucker-Prager and Mohr-Coulomb, clearly indicates that the strength development will be same, as long as angle of internal friction is the same. However, the stress-strain response depends on the liquid limit value. Greater the liquid limit greater will be the strain experienced by the soil to reach the strength for a given state.
- The stress-strain response predicted by the Drucker-Prager model is in agreement with the experimental results, though the strength value matches well with the Mohr-Coulomb model predictions. The strains predicted by Mohr-Coulomb model are conservative.
- The post peak softening in soils occur due to the presence of natural cementation and structure between soil grains and was not predicted by any of these models. However these models predict only elasto-plastic response of soils.
- These models do not capture the strain softening behavior which is the observed behavior for the case of natural soils.

REFERENCES

[1] Coombs, W. M., Crouch, R. S., and C. E. Heaney (2013), ´Observations on Mohr-Coulomb Plasticity under Plane Strain´, J. Eng. Mech., ASCE, Sep 2013.139:1218-1228.

[2] Clausen, J., Damkilde, L., and Andersen, L. (2006). "Efficient return algorithms for associated plasticity with multiple yield planes." Int. J. Numer. Methods Eng., 66(6), 1036–1059.

[3] Clausen, J., Damkilde, L., and Andersen, L. (2007). "An efficient return algorithm for non-associated plasticity with linear yield criteria in principal stress space." Comput. Struct., 85(23–24), 1795–1807.

[4] Wu, J.Y., Li, J., Faria, R., 2006. An energy release rate-based plastic-damage model for concrete. Int. J. Solids Struct. 43 (3–4), 583–612.

[5] Shao, C., Li, J., Wu, Y., 2009. Pseudo-potential of elastoplastic damage constitutive model and its application. Int. J. Solids Struct. 46 (21), 3894–3901.

[6] Voyiadjis, G.Z., Taqieddin, Z.N., Kattan, P.I., 2008. Anisotropic damage-plasticity model for concrete. Int. J. Plast. 24, 1946–1965.

[7] Al-Ajmi, A.M., Zimmerman, R.W., 2005. Relation between the Mogi and the Coulomb failure criteria. Int. J. Rock Mech. Miner. Sci. 42 (3), 431–439.

[8] Mao-Hong, Y., Guo-Wei, M., Hong-Fu, Q., Yong-Qiang, Z., (2006). Generalized Plasticity. Springer, Heidelberg/Berlin.

[9] Griffiths, D.V., Huang, J.S., (2009). Observations on the extended Matsuoka–Nakai failure criterion. Int. J. Numer. Anal. Meth. Geomech. 33 (17), 1189–1905.

[10] Chen, S. L., Y. N. Abousleiman, M. and K. K. Muraleetharan, F. (2012), Closed-Form Elastoplastic Solution for the Wellbore Problem in Strain Hardening/Softening Rock Formations, International Journal of Geomechanics, ASCE, July/August 2012.

[11] Drucker, D. C. and Prager, W. (1952), "Soil mechanics and plastic analysis or limit design", *Quart. Applied Math.* Vol. 10, No. 2, pp 157-165.

[12] Rakic, D., Zivkovic, M., Slavkovic, R. & Kojic, M. (2008), Stress Integration for the Drucker-Prager Material Model Without Hardening Using the Incremental Plasticity Theory, Journal of the Serbian Society for Computational Mechanics, Vol. 2, No. 1, 80-89.

[13] Atkinson, J.H. & Bransby, P.L. (1978), The mechanics of soils: an introduction to critical state soil mechanics.

[14] Suksun Horpibulsuk., Norihiro Miura. and Bergado, D. T. (2004), Undrained Shear Behavior of Cement Admixed Clay at High Water Content, Technical note, Journal of Geotechnical and Geoenvironmental Engineering, ASCE, Oct 2004, 1096-1105.

[15] Cheng Zhou., Jian-Hua Yin., Jun-Gao Zhu. and Chun-Man Cheng, (2005), Elastic Anisotropic Viscoplastic Modelling of the Strain-Rate-Dependent Stress-Strain Behavior of K_o-Consolidated Natural Marine Clays in Triaxial Shear Tests, International Journal of Geomechanics, ASCE, Sep 2005, 218-232.

[16] Futai, M. M., Almeida, S. S. and Lacerda, W. A. (2004), Yield, Strength and Critical State Behaviour of a Tropical Saturated Soil, Journal of Geotechnical and Geoenvironmental Engineering, ASCE, Nov 2004, 1169-1179.

[17] Burland, J. B., Rampello, S., Georgiannou, V. N. & Calabresi, G. (1996). A laboratory study of the strength of four stiff clays, Geotechnique 46, No. 3, 491-514.

[18] Balasubramaniam, A. S. and Chaudhry, A. R. (1978), Deformation and Strength Characteristics of Soft Bangkok Clay, Journal of Geotechnical Engineering Division, ASCE, 104, 1153-1167.

[19] Galal A. Hassaan, "Optimal Design of Machinery Shallow Foundations with Clay Soils", International Journal of Mechanical Engineering & Technology (IJMET), Volume 5, Issue 3, 2014, pp. 91 - 103, ISSN Print: 0976 – 6340, ISSN Online: 0976 – 6359.

[20] S. Ramesh Kumar and Dr. K.V.Krishna Reddy, "An Experimental Investigation on Stabilization of Medium Plastic Clay Soil with Bituminous Emulsion", International Journal of Civil Engineering & Technology (IJCIET), Volume 5, Issue 1, 2014, pp. 61 - 65, ISSN Print: 0976 – 6308, ISSN Online: 0976 – 6316.

[21] Mohammed Fadhil Obaid, Dr. V. C. Agarwal, Prabhat Kumar Sinha and Ahmed Neamah Naji, "The Influence of Organic Solutes on the Geotechnical Properties of Extremely Plastic Clayey Soils", International Journal of Civil Engineering & Technology (IJCIET), Volume 5, Issue 3, 2014, pp. 83 - 91, ISSN Print: 0976 – 6308, ISSN Online: 0976 – 6316.

Appendix

a) Drucker-Prager Model in p-q space

$$F(0) = \sqrt{J_{2D}} - \alpha J_1 - k \quad (a.1)$$

Where,

$$J_1 = \sigma_1 + \sigma_2 + \sigma_3 = \sigma_1 + 2\sigma_3 = 3p \quad (a.2)$$

$$J_{2D} = (1/6)\left((\sigma_1 - \sigma_2)^2 + (\sigma_2 - \sigma_3)^2 + (\sigma_1 - \sigma_3)^2\right) = (1/3)(\sigma_1 - \sigma_3)^2 = q^2/3 \quad (a.3)$$

Substitute (a.2) and (a.3) in (a.1)

$$F(0) = \sqrt{(q^2/3)} - 3\alpha p - k \quad (a.4)$$

Where,

$$k = \frac{6c\cos\phi}{\sqrt{3}(3 - \sin\phi)}$$

$$\alpha = \frac{2\sin\phi}{\sqrt{3}(3 - \sin\phi)}$$

Consistency condition, dF = 0

$$\frac{\partial F}{\partial p}dp + \frac{\partial F}{\partial q}dq = 0 \quad (a.5)$$

$dp = K\,(d\epsilon_v - d\epsilon_v^p)$ (a.6)

$dq = 3G\,(d\epsilon_s - d\epsilon_s^p)$ (a.7)

$d\epsilon_v^p = d\lambda\,(\partial F / \partial p)$ (a.8)

$d\epsilon_s^p = d\lambda\,(\partial F / \partial q)$ (a.9)

Substitute (a.6) to (a.9) in (a.5)

$$\frac{\partial F}{\partial p} K\, d\epsilon_v - \frac{\partial F}{\partial p} K\, d\lambda \frac{\partial F}{\partial p} + \frac{\partial F}{\partial q} 3G\, d\epsilon_s - \frac{\partial F}{\partial q} 3G\, d\lambda \frac{\partial F}{\partial q} = 0 \quad \text{(a.10)}$$

$$d\lambda = \frac{\frac{\partial F}{\partial p} K\, d\epsilon_v + \frac{\partial F}{\partial q} 3G\, d\epsilon_s}{\frac{\partial F}{\partial p} K \frac{\partial F}{\partial p} + \frac{\partial F}{\partial q} 3G \frac{\partial F}{\partial q}} \quad \text{(a.11)}$$

But,

$(\partial F / \partial p) = -3\alpha$

$(\partial F / \partial q) = 1/\sqrt{3}$

Therefore,

$$d\lambda = \frac{-3\alpha K\, d\epsilon_v + \sqrt{3} G\, d\epsilon_s}{9\alpha^2 K + G} \quad \text{(a.12)}$$

$d\epsilon_v^p = -3\alpha\, d\lambda$ (a.13)

$d\epsilon_s^p = d\lambda/\sqrt{3}$ (a.14)

Substitute (a.12) to (a.14) in (a.6) and (a.7)

$dp = K\,(d\epsilon_v + 3\alpha\, d\lambda)$

$$dp = K\left[d\epsilon_v + 3\alpha\left(\frac{-3\alpha K\, d\epsilon_v + \sqrt{3} G\, d\epsilon_s}{9\alpha^2 K + G}\right)\right]$$

$$dp = K\, d\epsilon_v - \frac{9\alpha^2 K^2}{9\alpha^2 K + G} d\epsilon_v + \frac{3\sqrt{3}\alpha K G}{9\alpha^2 K + G} d\epsilon_s$$

$$dp = \left[K - \frac{9\alpha^2 K^2}{9\alpha^2 K + G}\right] d\epsilon_v + \left[\frac{3\sqrt{3}\alpha K G}{9\alpha^2 K + G}\right] d\epsilon_s \quad \text{(a.15)}$$

and

$dq = 3G\,(d\epsilon_s - (1/\sqrt{3})d\lambda)$

$$dq = 3G\left[d\epsilon_s - \frac{1}{\sqrt{3}}\left(\frac{-3\alpha K\, d\epsilon_v + \sqrt{3} G\, d\epsilon_s}{9\alpha^2 K + G}\right)\right]$$

$$dq = 3G\, d\epsilon_s + \frac{3\sqrt{3}\alpha K G}{9\alpha^2 K + G} d\epsilon_v - \frac{3G^2}{9\alpha^2 K + G} d\epsilon_s$$

$$dq = \left[\frac{3\sqrt{3}\alpha KG}{9\alpha^2 K + G}\right] d\epsilon_v + \left[3G - \frac{3G^2}{9\alpha^2 K + G}\right] d\epsilon_s \quad \text{(a.16)}$$

Equations (a.15) and (a.16) can be written in the matrix form as,

$$\begin{bmatrix} dp \\ dq \end{bmatrix} = \begin{bmatrix} K - \frac{9\alpha^2 K^2}{9\alpha^2 K + G} & \frac{3\sqrt{3}\alpha KG}{9\alpha^2 K + G} \\ \frac{3\sqrt{3}\alpha KG}{9\alpha^2 K + G} & 3G - \frac{3G^2}{9\alpha^2 K + G} \end{bmatrix} \begin{bmatrix} d\epsilon_v \\ d\epsilon_s \end{bmatrix} \quad \text{(a.17)}$$

b) Mohr-Coulomb Model in p-q space

$F(0) = (\sigma_1 - \sigma_3) - (\sigma_1 + \sigma_3)\sin\phi - 2c\cos\phi$ (b.1)

$p = (\sigma_1 + \sigma_3)/2 \Rightarrow \sigma_1 = 2p - \sigma_3$ (b.2)

$q = (\sigma_1 - \sigma_3)/2 \Rightarrow \sigma_3 = \sigma_1 - 2q$ (b.3)

From (c.2) and (c.3),

$\sigma_1 = 2p - (\sigma_1 - 2q) = p + q$ (b.4)

$\sigma_3 = p + q - 2q = p - q$ (b.5)

$\sigma_1 + \sigma_3 = 2p$ (b.6)

$\sigma_1 - \sigma_3 = 2q$ (b.7)

Substitute (c.6) and (c.7) in (c.1)

$F(0) = 2q - 2p\sin\phi - 2c\cos\phi = 0$

$F(0) = q - p\sin\phi - c\cos\phi = 0$ (b.8)

Consistency condition, dF = 0

$$\frac{\partial F}{\partial p} dp + \frac{\partial F}{\partial q} dq = 0 \quad \text{(b.9)}$$

$dp = K(d\epsilon_v - d\epsilon_v^p)$ (b.10)

$dq = 3G(d\epsilon_s - d\epsilon_s^p)$ (b.11)

$d\epsilon_v^p = d\lambda(\partial F / \partial p)$ (b.12)

$d\epsilon_s^p = d\lambda(\partial F / \partial q)$ (b.13)

Substitute (c.10) to (c.13) in (c.9)

$$\frac{\partial F}{\partial p} K d\epsilon_v - \frac{\partial F}{\partial p} K d\lambda \frac{\partial F}{\partial p} + \frac{\partial F}{\partial q} 3G d\epsilon_s - \frac{\partial F}{\partial q} 3G d\lambda \frac{\partial F}{\partial q} = 0 \quad \text{(b.14)}$$

$$d\lambda = \frac{\frac{\partial F}{\partial p} K d\epsilon_v + \frac{\partial F}{\partial q} 3G d\epsilon_s}{\frac{\partial F}{\partial p} K \frac{\partial F}{\partial p} + \frac{\partial F}{\partial q} 3G \frac{\partial F}{\partial q}} \quad \text{(b.15)}$$

But,

$(\partial F / \partial p) = -\sin\phi$

$(\partial F / \partial q) = 1$

Therefore,

$$d\lambda = \frac{-K \sin\phi \, d\epsilon_v + 3G \, d\epsilon_s}{K \sin^2\phi + 3G} \tag{b.16}$$

$d\epsilon_v^p = -\, d\lambda \sin\phi$ (b.17)

$d\epsilon_s^p = d\lambda$ (b.18)

Substitute (c.16) to (c.18) in (c.10) and (c.11)

$dp = K (d\epsilon_v + d\lambda \sin\phi)$

$$dp = K \left[d\epsilon_v + \frac{-K \sin\phi \, d\epsilon_v + 3G \, d\epsilon_s}{K \sin^2\phi + 3G} \sin\phi \right]$$

$$dp = K \, d\epsilon_v - \frac{K^2 \sin^2\phi}{K \sin^2\phi + 3G} d\epsilon_v + \frac{3GK \sin\phi}{K \sin^2\phi + 3G} d\epsilon_s$$

$$dp = \left[K - \frac{K^2 \sin^2\phi}{K \sin^2\phi + 3G} \right] d\epsilon_v + \left[\frac{3GK \sin\phi}{K \sin^2\phi + 3G} \right] d\epsilon_s \tag{b.19}$$

and

$dq = 3G (d\epsilon_s - d\lambda)$

$$dq = 3G \left[d\epsilon_s - \frac{-K \sin\phi \, d\epsilon_v + 3G \, d\epsilon_s}{K \sin^2\phi + 3G} \right]$$

$$dq = 3G \, d\epsilon_s + \frac{3GK \sin\phi}{K \sin^2\phi + 3G} d\epsilon_v - \frac{9G^2}{K \sin^2\phi + 3G} d\epsilon_s$$

$$dq = \left[\frac{3GK \sin\phi}{K \sin^2\phi + 3G} \right] d\epsilon_v + \left[3G - \frac{9G^2}{K \sin^2\phi + 3G} \right] d\epsilon_s \tag{b.20}$$

Equations (c.19) and (c.20) can be written in the matrix form as,

$$\begin{bmatrix} dp \\ dq \end{bmatrix} = \begin{bmatrix} K - \frac{K^2 \sin^2\phi}{K \sin^2\phi + 3G} & \frac{3GK \sin\phi}{K \sin^2\phi + 3G} \\ \frac{3GK \sin\phi}{K \sin^2\phi + 3G} & 3G - \frac{9G^2}{K \sin^2\phi + 3G} \end{bmatrix} \begin{bmatrix} d\epsilon_v \\ d\epsilon_s \end{bmatrix} \tag{b.21}$$